Surv. Math. Ind. (1996) 6: 75–107

Surveys on Mathematics for Industry

Stability and instability in evaporating two-phase flows

Christopher J. Aldridge, Glasgow, and **Andrew C. Fowler**, Oxford

Dedicated to the memory of Alan Tayler

Summary. We review the analysis of linear and nonlinear stability in heated two-phase flows in a channel, with particular reference to the operation of boilers. Two main classes of instability are static (or Ledinegg) instability, wherein a small perturbation leads to a flow excursion to a different operating state, and oscillatory instability, also called density-wave oscillations. These instabilities correspond respectively to exchange of stability and Hopf bifurcation. We illustrate this existence in an asymptotically reduced two-fluid mathematical model, and we compare these results to those of other authors.

AMS Subject Classification: 76E99, 76T05, 80A20

Keywords: Two-phase flow; Evaporation; Instability; Density-wave oscillations; Ledinegg instability.

1 Introduction

The Oxford Study Groups for Industry were formed by Alan Tayler in the late 1960s, and one of the problems brought to Oxford in 1973 or thereabouts was from Babcock and Wilcox in Scotland, who were concerned with instabilities in heat exchangers. One of us (A.C.F.) began his research career by writing an M.Sc. dissertation on this topic under Alan's guidance, which was subsequently published [23]. There the matter rested until 1989, when the first author began his doctoral research in Oxford on an expanded study of the same basic problem, under the second's direction. This thesis has just appeared [3], and in this paper we survey the field of study and illustrate it with some results of this recent work.

Thermally-induced two-phase flow instabilities are an important problem in the design and operation of industrial systems such as heat exchangers and steam generators. Two-phase flow generally refers to the flow of a mixture containing two distinct phases, and is commonly encountered in industrial processes. In particular, boiling and condensing flows of liquid and gas are prevalent within the power, heat transfer and process industries. In the steam generator of a power station, for example, water is pumped through a heated channel and boils, giving rise to a region of two-phase flow, and after complete evaporation, the flow is of superheated steam. Similar flows occur in the coolant loops in nuclear reactors, liquid fuelled rocket engines and cryogenic equipment.

Industrial systems involving boiling two-phase flow are prone to a variety of different types of instabilities, which are undesirable for several reasons. A system is difficult to control if oscillations are present, and mechanical vibrations may damage components. Worst of all, the local heat transfer characteristics of the flow may be affected. If the heated surface loses direct contact with the liquid, the heat

transfer from the wall is dramatically reduced, and the wall temperature increases. This situation is commonly referred to as burnout, and can lead to immediate failure of the tube. If this happens periodically, then enhanced corrosion may occur in steel-walled tubes [5]. Each rise in wall temperature sets up stresses within the layer of magnetite on the interior of the tube, which breaks down and leaves the wall; when the flow returns to original conditions, a new layer grows using iron from the tube wall. Repeated cycles of this process then lead to serious corrosion. Alternatively, higher frequency flow oscillations may cause damage, as oscillations in the wall temperature can lead to thermal fatigue.

In view of the potential problems caused by two-phase flow instabilities, there is a need to understand and predict these phenomena. In particular, the growth of nuclear power over the last three decades has led to a considerable amount of research aimed at ensuring the safe operation of coolant systems within nuclear plants. Much of this has involved the construction of complicated models, which couple the coolant flow and heat transfer with the reactor dynamics, and the development of large computer codes to solve the model equations. At the same time, many analyses have been published which investigate the onset of two-phase flow instabilities using simpler models. In this paper, we review previous work of the latter type on the stability of two-phase flows, as well as presenting our own more recent results.

1.1 Flow regimes

The flow of a gas-liquid mixture along a pipe is characterised by a variety of possible configurations which the phases may adopt. Such configurations are traditionally classified into "flow regimes", or "flow patterns", and are an important constitutent of two-phase flow modelling. A number of reviews of flow regimes have appeared in text-books on two-phase flows [15, 27, 28, 48]. The classification of the interfacial distribution into distinct regimes is necessarily a subjective exercise, however, there are several main generally accepted patterns, which for vertical upflow are illustrated in Fig. 1.

The particular regime present in a flow depends on a number of factors, such as the pipe geometry and orientation, and the flow rates of the phases. Much experimental effort has been directed towards identifying flow regimes in various situations and quantifying their dependence on system parameters; laboratory techniques range from photography to X- and gamma-ray absorption. This has led to the construction of flow maps, two-dimensional graphs (with various phasic quantities as coordinates) which are delineated into areas associated with different flow patterns. Alternatively, maps may be derived by modelling the transitions between flow patterns. We now outline the regimes present in a two-phase flow along a heated pipe.

When evaporation begins, small bubbles are nucleated at the walls of the tube, detach and move into the bulk fluid. If the heat flux is relatively high, this may occur when the (local) temperature of the liquid is below saturation (subcooled boiling). For lower heat fluxes, the liquid may become superheated before nucleation occurs. Along the length of two-phase flow, nucleate boiling gives way to direct

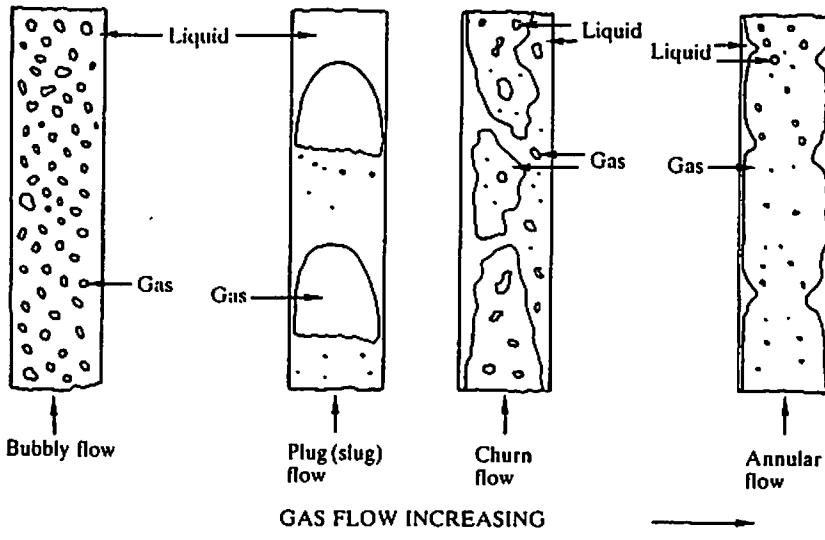

Fig. 1. Flow regimes in vertical upflow in a tube (from Whalley [48], p. 5, by permission of Oxford University Press)

evaporation at the interface as the chief mechanism of vapour generation. When bubbles of gas flow in a liquid continuum, the regime is known as *bubbly flow*. As boiling proceeds larger bubbles are formed, through coalescence or evaporation at the interface, and there is a transition to the regime known as *slug flow*. In this regime, the gas flows mainly in large bullet-shaped voids known as "plugs", separated by "slugs" of liquid. Smaller gas bubbles are distributed throughout the liquid. As the gas flow rate increases along the tube, the structure of the plugs is lost, and the flow evolves to the unstable *churn flow* regime. Eventually the *annular flow* regime is reached, in which the liquid flows as a film at the tube wall, surrounding a central gas core. Droplets of liquid are entrained from and are redeposited on the relatively slow moving film.

The liquid flow in the film decreases due to evaporation and entrainment. Eventually the film may completely evaporate (leading to "dryout"), though entrained droplets may survive beyond this point.

1.2 Two-phase flow instabilities

Two-phase flow instabilities have been the subject of a number of extensive reviews [5, 7, 9, 31, 34] which describe the various instability phenomena, and summarise the many experimental and theoretical investigations in this area. There is a traditional classification into "static" and "dynamic" instabilities. When a perturbation to an unstable steady state leads to a departure towards a stable steady state, this is termed a static instability. Dynamic instabilities refer to the case when the perturbation leads to sustained oscillations in the flow. Thus these two classes simply correspond to the presence of disturbances proportional to $e^{\sigma t}$, where σ is real and positive (static) or complex conjugate with positive real part (dynamic).

Static instabilities describe several flow and heat transfer phenomena, including Ledinegg instability, flow regime transition, and burnout. *Ledinegg instability* is named after the author of the first successful analysis [36]. When an initially subcooled liquid flows through a boiling channel, the steady state dependence of the pressure drop on the inlet velocity can admit multiple solutions for the flow. The large-scale drift of the flow from an unstable steady state towards a stable steady state is known as a Ledinegg instability, or "flow excursion".

The particular flow regime which exists along a channel is determined by the phasic flow rate and other parameters. Hence when the flow is close to transition conditions, a small disturbance may lead to interfacial instabilities and hence a *flow regime transition*. An analogous situation involving heat transfer at the wall is known as *burnout*. Under certain conditions, a disturbance to the flow may lead to a change in the character of evaporation, with the heated surface no longer in contact with the liquid phase (due to the formation of an insulating film of gas at the wall). Hence a small change in the flow can reduce the heat transfer coefficient by a factor of 100 [48].

The most common forms of dynamic instabilities are density-wave oscillations, pressure-drop oscillations, and acoustic oscillations. The first two of these phenomena involve oscillations of the inlet velocity due to the single-phase and two-phase pressure gradients; the terminology in both cases is due to Stenning and Veziroglu (reported in [34]). *Density-wave oscillations* have relatively low frequency (~ 1 Hz), and involve waves of *mixture* density propagating along the tube. Thus "density waves" do not result from compressibility of the individual phases, but are associated with variations in the void fraction (an increase in the proportion of the gas giving a lower mixture density). The terms "concentration waves" and "void waves" are hence also used to describe this phenomenon. Such waves may occur along a channel while the total pressure drop is kept constant because the (subcooled and two-phase) components of the pressure drop oscillate out of phase.

Pressure-drop oscillations arise when a compressible volume (a "surge tank") is connected upstream of the heated channel. The onset of oscillations follows a Ledinegg instability; hence these phenomena are associated in the literature with the same range of operating conditions. The compressibility of the air in the surge tank (and vapour in the tube) allows hysteresis of the system around the inlet velocity–pressure drop curve, at a relatively very low frequency (~ 0.1 Hz). *Acoustic oscillations* involve the propagation of pressure waves at the speed of sound of the two-phase mixture. These high frequency (~ 10–100 Hz) oscillations do not generally lead to problematic pressure or flow fluctuations.

2 Two-phase flow models

In the last thirty years many analyses of two-phase flow instabilities have been published. The various two-phase flow models employed divide into three types: homogeneous, drift-flux, and two-fluid models. Each approach is based on one-dimensional conservation equations for mass, momentum and energy, for the mixture (homogeneous model), the individual phases (two-fluid model), or a

combination of both (drift-flux model). We describe these different models below. First of all, we discuss two-phase flow modelling in general, and in particular focus on the use of averaging methods.

In the development of models for two-phase flows, a number of general approaches may be used. Ishii and Kokamustafaogullari [32] discuss some of the methodologies. Since a two-phase flow is composed of distinct single-phase regions separated by moving interfaces, a possible approach is to formulate standard single-phase conservation laws for these regions with boundary conditions at the interfaces (whose positions are unknown). Solving such a *multi-boundary problem* is however unfeasible for all but the simplest situations. In any case, in order to predict two-phase instabilities, we are interested in a description of the mean flow rather than the microscopic features.

There are three main macroscopic approaches. The first is based on an assumption of *interacting continua*: each "point" in the two-phase flow is occupied simultaneously by both phases. Such models were first developed for mixtures of gases (with no interfaces), and later extended to more general cases. However, since we wish to describe discrete single-phase regions divided by interfaces, the continuum assumption made here is not well founded. Moreover, the essential characteristic of two-phase flow—the interfaces—are ignored. A second macroscopic approach is based on a *control volume*, either in the mixture or in each phase, for which balance laws are written. Usually models of this type are one-dimensional, the flow being modelled as separated phases divided by a moving interface. This approach has been used successfully for a limited range of separated flows, such as annular flow.

The two approaches described above essentially involve the postulation of a model. A third, more rational, method is to formulate a macroscopic model through the rigorous use of *averaging* techniques, as suggested by the averaging approach to turbulence [29]. As Drew and Lahey [19] point out, while the unnecessary details are filtered out during the averaging process, we gain undetermined terms in the averaged equations, which represent the effects of the lost information. Hence constitutive relations must be prescribed for these terms. Drew [18] cites some advantages of postulational and averaging approaches. An obvious advantage of the former is that there is no concern over the detailed averaging process. However, the averaged approach shows the development of terms in the macroscopic equations from microscopic quantities, for example, macroscopic stresses arise both from microscopic stresses and also from velocity fluctuations. Furthermore, the resulting macroscopic variables are related to the microscopic variables, which can assist in the formulation of constitutive relations. We now discuss some of the averaging methods that have been proposed for two-phase flow modelling.

2.1 Averaging methods

Time and space averaging

The first averaged two-phase flow models to appear in the literature were based on time and space averaging. In this process, local instantaneous variables are

replaced by variables smoothed over regions in space and/or time, under the assumption that there exist intermediate scales much larger than the scales of microscopic variation, but much smaller than the scales of interest. Spatial averaging is founded on a length scale L satisfying $l \ll L \ll L_s$, where l and L_s are the microscopic and system length scales, respectively. Then a volume average may be introduced as [18]

$$\langle f(\mathbf{x},t)\rangle = \frac{1}{L^3}\int_{x_1-L/2}^{x_1+L/2}\int_{x_2-L/2}^{x_2+L/2}\int_{x_3-L/2}^{x_3+L/2} f(\mathbf{x}',t)\,\mathrm{d}x_1\,\mathrm{d}x_2\,\mathrm{d}x_3\,. \tag{2.1}$$

Similarly a time-average approach is based on a time scale T satisfying $t^* \ll T \ll T_s$, where t^* and T_s are the turbulent and system time scales, respectively. Ishii [30] derived averaged two-phase flow equations using the time average

$$\langle f(\mathbf{x},t)\rangle = \frac{1}{T}\int_t^{t+T} f(\mathbf{x}',t)\,\mathrm{d}t\,. \tag{2.2}$$

Averaged two-phase flow equations were first developed to describe the motion of solid-liquid mixtures. Frankl [24] modelled the flow of suspended sediments using the combined space-time average

$$\langle f(\bar{\mathbf{x}},\bar{t})\rangle = \frac{\iiint_{Z(\bar{\mathbf{x}},\bar{t})} f(\mathbf{x},t)\,\mathrm{d}x_1\,\mathrm{d}x_2\,\mathrm{d}x_3\,\mathrm{d}t}{\iiint_{Z(\bar{\mathbf{x}},\bar{t})}\mathrm{d}x_1\,\mathrm{d}x_2\,\mathrm{d}x_3\,\mathrm{d}t}, \tag{2.3}$$

over an averaging region $Z(\bar{\mathbf{x}},\bar{t})$ given by

$$\sum_{i=1}^{3}(x_i-\bar{x}_i)^2 \le r^2, \quad |t-\bar{t}| < \Delta t\,. \tag{2.4}$$

Anderson and Jackson [4] derived a continuum model for a fluidised bed using a weighted volume average, defining "local mean voidage" by

$$\varepsilon(\mathbf{x},t) = \int_{V_f(t)} g(|\mathbf{x}-\mathbf{y}|)\,\mathrm{d}V_y, \tag{2.5}$$

where the integral is taken over all the points y occupied by the fluid at time t, $\mathrm{d}V_y$ is an element of volume in the neighbourhood of y, and $g(\cdot)$ is a weighting function.

A general model for two-phase media was derived by Drew [17] based on an averaging process involving two integrations over spheres in three-space, and two integrations in time, to give differentiability. Averaged quantities were defined using proper weightings with void fractions and densities: thus an averaged velocity is defined as the ratio of an averaged momentum and an averaged density. This reflects the way these quantities are measured and how they appear in the equations. Whitaker [49] derived general transport equations for multiphase flow using three different volume averages. A spatial average, phase average, and

intrinsic phase average were defined respectively by

$$\langle \psi \rangle = \frac{1}{V} \int_V \psi \, dV, \tag{2.6}$$

$$\langle \psi \rangle^\alpha = \frac{1}{V} \int_{V_\alpha(t)} \psi_\alpha \, dV, \tag{2.7}$$

$$\langle \psi_\alpha \rangle^\alpha = \frac{1}{V_\alpha(t)} \int_{V_\alpha(t)} \psi \, dV, \tag{2.8}$$

where ψ_α is ψ restricted to phase α, V is the volume surrounding a point, and V_α that part of V occupied by phase α. Whitaker derived a phase-averaged general transport equation, and recast some of the terms as intrinsic phase averages by introducing the volume fraction $\varepsilon_\alpha = V_\alpha/V$. The resulting equations are similar to those of Drew [17], though they include two types of averages. Further models based on volume averaging were developed by Nigmatulin [37] and Hassanizadeh and Gray [26].

A systematic development of space and time-averaged equations is presented by Delhaye [16] and Bouré and Delhaye [10]. The time average is taken over an interval $[T] := [t - T/2, t + T/2]$, as

$$\langle f_k \rangle = \frac{1}{T_k} \int_{[T_k]} f_k \, dt. \tag{2.9}$$

Here f_k is a quantity restricted to phase k, $[T_k]$ is the subset of residence time-intervals of phase k in $[T]$, and T_k is the cumulative residence time of phase k in $[T]$.

Ensemble averaging

Buyevich and Shchelchkova [12] discuss the modelling of dense suspensions, and suggest that methods of time and space averaging have a "principal defect". In addition to volume averages, the resulting equations usually contain quantities obtained by averaging over differently orientated physical surfaces. Hence extra ergodic hypotheses are needed to relate these quantities. This motivates an alternative, statistical averaging approach, based on the concept of an *ensemble*, or set of possible states of the system. According to the above authors, the necessity to use ensemble averaging (rather than space and time averaging) was first discussed by Batchelor [6], in the context of modelling suspensions. Batchelor notes that the exact location of particles is different for different realisations of the system with the same macroscopic boundary conditions. An ensemble is defined as a large number of such realisations; an ensemble average is then simply an average over the values taken by some physical quantity over the set of realisations.

Drew and Wood [20] present a rigorous derivation of two-phase flow equations, based on an ensemble average defined by

$$\bar{f}(\mathbf{x}, t) = \int_M f(\mathbf{x}, t; \mu) \, dm(\mu). \tag{2.10}$$

Here M is the set of all processes, or ensemble, μ is a specific process in the ensemble, $dm(\mu)$ is a measure (probability) of observing process μ, and f is some quantity associated with μ. In stationary flows (corresponding to steady averaged variables), the ensemble average may be replaced by a time average,

$$\bar{f}(\mathbf{x}) = \frac{1}{T}\int_{t-T}^{t} f(\mathbf{x}, t-\tau; \mu^*)\,d\tau. \tag{2.11}$$

Similarly, in the case of spatially homogeneous flows, the ensemble average may be approximated by a volume average. In these cases, averaged values may be obtained via one detailed observation rather than sampling a whole ensemble of flows. Drew and Wood suggest that the ensemble averaging is the "fundamental" approach, while space and time averaging are only appropriate as approximations in certain cases.

Averaging procedure

We now briefly outline the averaging process presented by Drew [18] and Drew and Wood [20]. The development of an averaged model from the microscopic equations begins with the introduction of an indicator function X_k for each phase k. This function is defined by $X_k(\mathbf{x}, t) = 1$ if $\mathbf{x}$ is in phase k at time t, otherwise $X_k(\mathbf{x}, t) = 0$, and is considered as a generalised function, which enables the subsequent use of integration by parts. The general conservation equation (describing the transport of mass, momentum, and energy) may be written as

$$\frac{\partial}{\partial t}(\rho\psi) + \nabla\cdot(\rho\psi\mathbf{v}) = -\nabla\cdot\mathbf{J} + \rho f, \tag{2.12}$$

where $\mathbf{J}$ is the flux and f the source density of the conserved quantity ψ, ρ is the density, and $\mathbf{v}$ is the velocity. Equation (2.12) is first multiplied by X_k, and then averaged (over space, time, or an ensemble). Assuming that $\overline{\partial f/\partial t} = \partial\bar{f}/\partial t$ and $\overline{\nabla f} = \nabla\bar{f}$, where the overline denotes an average, this leads to

$$\frac{\partial}{\partial t}\overline{(X_k\rho\psi)} + \nabla\cdot\overline{(X_k\rho\psi\mathbf{v})} = -\nabla\cdot\overline{(X_k\mathbf{J})} + \overline{X_k\rho f} + \overline{(\rho\psi(\mathbf{v}-\mathbf{v}_i)+\mathbf{J})\cdot\nabla X_k}. \tag{2.13}$$

Here $\mathbf{v}_i$ is the velocity of the moving interface. The last term is the interfacial source of ψ, since for a general vector field $\mathbf{y}$, $\overline{\mathbf{y}\cdot\nabla X_k}$ represents the surface average of $-\mathbf{y}\cdot\mathbf{n}$, where $\mathbf{n}$ is the unit normal directed away from phase k.

For example, conservation of mass is given by (2.12) with $\psi = 1, \mathbf{J} = \mathbf{0}$ and $f = 0$. In this case, (2.13) gives

$$\frac{\partial}{\partial t}\overline{(X_k\rho)} + \nabla\cdot\overline{(X_k\rho\mathbf{v})} = \overline{\rho(\mathbf{v}-\mathbf{v}_i)\cdot\nabla X_k}. \tag{2.14}$$

This motivates the definition of average volume fraction, density, and velocity by

$$\bar{\alpha}_k = \overline{X_k}, \tag{2.15}$$

$$\bar{\rho}_k^x = \overline{X_k \rho}/\alpha_k, \tag{2.16}$$

$$\bar{\mathbf{v}}_k^{x\rho} = \overline{X_k \rho \mathbf{v}}/\alpha_k \rho_k. \tag{2.17}$$

Denoting the right-hand side of (2.14) by $\bar{\Gamma}_k$, representing mass source due to phase change, (2.14) gives conservation of mass for each phase k as

$$\frac{\partial}{\partial t}(\bar{\alpha}_k \bar{\rho}_k^x) + \nabla\cdot(\bar{\alpha}_k \bar{\rho}_k^x \bar{\mathbf{v}}_k^{x\rho}) = \bar{\Gamma}_k. \tag{2.18}$$

In this way, we obtain a set of averaged three-dimensional conservation equations for the mass, momentum and energy of the two phases. These are accompanied by averaged jump conditions for the conserved quantities at the interface.

For two-phase flow along a channel, a one-dimensional model is appropriate, hence the equations are further averaged over a channel cross-section. We define the area average as

$$\langle \bar{f}(\mathbf{x}, t)\rangle = \frac{1}{A(z)} \int_{A(z)} \bar{f}(\mathbf{x}, t)\, \mathrm{d}A, \tag{2.19}$$

where A is the cross-sectional area and z the coordinate along the axis of the channel. The one-dimensional model is formed from the area-averaged mass and energy equations and the axial component of the momentum equation. Area-averaged variables, such as the volume fractions, densities and velocities of the phases, are defined in a similar way to before, based on the structure of the averaged terms arising in the equations. The equations also include interfacially-averaged variables, for example the mass source at the interface. Area-averaging the gradient terms in the equations also creates perimeter-averaged quantities, such as the stress at the wall. The undetermined terms arising from the twin averaging processes (such as the stresses) must be prescribed by constitutive relations.

2.2 Three different models

Homogeneous model

The simplest way to model two-phase flow is to describe the mixture as a homogeneous single-phase fluid. Early studies of two-phase flow instabilities [8, 14] were based on such a homogeneous model. In this model there is one density, namely the mixture density, one velocity, one pressure and one enthalpy. The gas volume fraction does not explicitly appear, though it essentially determines the mixture density. Consequently there is no need to do any (volume, time, or ensemble) averaging to write down the model, as the equations are identical to those of single-phase flow. However, the model may be obtained from the averaged equations by adding the corresponding phasic equations, and defining new mixture

variables in terms of the (averaged) phasic variables. For example, let ρ_g and ρ_l be the gas and liquid densities, and α be the volume fraction of gas (known as the 'void fraction'). Then the mixture density is defined as

$$\rho_m = \alpha\rho_g + (1-\alpha)\rho_l. \tag{2.20}$$

The mixture velocity is defined as the mass flux of the mixture divided by its density,

$$u_m = (\alpha\rho_g v + (1-\alpha)\rho_l u)/\rho_m, \tag{2.21}$$

where v and u are the gas and liquid velocities; and the mixture enthalpy is defined similarly,

$$h_m = (\alpha\rho_g h_g + (1-\alpha)\rho_l h_l)/\rho_m, \tag{2.22}$$

where h_g and h_l are the gas and liquid enthalpies. The model equations take the form [14]

$$\frac{\partial\rho_m}{\partial t} + \frac{\partial}{\partial z}(\rho_m u_m) = 0, \tag{2.23}$$

$$\frac{\partial}{\partial t}(\rho_m u_m) + \frac{\partial}{\partial z}(\rho_m u_m^2) = -\frac{\partial p}{\partial z} - F_{mw} - \rho_m g, \tag{2.24}$$

$$\rho_m\left(\frac{\partial h_m}{\partial t} + u_m\frac{\partial h_m}{\partial z}\right) = \frac{Q}{A}. \tag{2.25}$$

Here p is the pressure, F_{mw} is the stress on the mixture due to the tube walls, g is the gravitational constant, h_m is the mixture enthalpy, Q is the heat input per unit time per unit length, and A is the cross-sectional area (assumed to be constant). In addition an equation of state is prescribed for the mixture, constituting ρ_m in terms of p and h_m.

The chief advantage of the homogeneous model is its simplicity: there are no phasic interaction terms to be constituted (as these terms cancel out when we consider the mixture as a whole). However, implicit in the model is the assumption that the phasic velocities are equal, whereas in practice there may be significant *slip* between the gas and liquid (particularly in annular flow). Hence the homogeneous model is most appropriate when the phases are strongly coupled, such as in bubbly flow.

Drift-flux model

The drift-flux model [51] allows slip between the phases by prescribing the velocity of the gas relative to the motion of the mixture. The volumetric flux j of the mixture is given by

$$j = \alpha v + (1-\alpha)u; \tag{2.26}$$

the *drift velocity* of the gas is defined as

$$V_{gj} := v - j = (1-\alpha)(v-u). \tag{2.27}$$

If the drift velocity is zero, then $v = u = j = u_m$. Otherwise if $V_{gj} \neq 0$, $j \neq u_m$, thus the velocities of the centre of volume and centre of mass of the mixture are different. In annular flow, for example, the velocity of the centre of volume is approximately the velocity of the gas, which has the larger specific volume, while the velocity of the centre of mass will be approximately the velocity of the denser liquid. In the drift-flux model, V_{gj} is prescribed as a function of the independent variables and system parameters. Correlations for V_{gj} have been obtained by experimental observation and theoretical analyses for a range of flow regimes.

The drift-flux model presented by Zuber [51] considers a boiling two-phase flow, in which the liquid is in thermal non-equilibrium and the gas incompressible and at saturation temperature. The model adds conservation of mass for the gas to the three mixture equations used in the homogeneous model, with extra terms in the momentum and enthalpy equations due to slip. The equations are

$$\frac{\partial}{\partial t}(\alpha\rho_g) + \frac{\partial}{\partial z}[\alpha\rho_g(j + V_{gj})] = \Gamma_g, \tag{2.28}$$

$$\frac{\partial\rho_m}{\partial t} + \frac{\partial}{\partial z}(\rho_m u_m) = 0, \tag{2.29}$$

$$\rho_m\left\{\frac{\partial\rho_m}{\partial t} + u_m\frac{\partial\rho_m}{\partial z}\right\} = -\frac{\partial p}{\partial z} - F_{mw} - \rho_m g - \frac{\partial}{\partial z}\left\{\frac{\rho_l - \rho_m}{\rho_m - \rho_g}\frac{\rho_l\rho_g}{\rho_m}V_{gj}^2\right\}, \tag{2.30}$$

$$\rho_m\left(\frac{\partial h_m}{\partial t} + u_m\frac{\partial h_m}{\partial z}\right) = \frac{Q}{A} - \frac{\partial}{\partial z}\left\{\frac{\rho_l - \rho_m}{\rho_m}\frac{\rho_l\rho_g}{\rho_l - \rho_g}V_{gj}(h_g - h_l)\right\} + \frac{\partial p}{\partial t}. \tag{2.31}$$

To these four partial differential equations are added the equation of state for the liquid, $\rho_l = \rho_l(h_l, p)$; definitions of mixture density (2.20), and mixture enthalpy (2.22); the prescription of the drift velocity, $V_{gj} = V_{gj}(\alpha, u_m, p, \ldots)$; the relationship linking j, V_{gj} and u_m,

$$j = u_m + \alpha[(\rho_l - \rho_g)/\rho_m]\,V_{gj}; \tag{2.32}$$

and appropriate constitutive relations as usual. The drift-flux model has been thoroughly studied in gravity-dominated, vertical flows, where it is found to work well [20].

Two-fluid model

The two-fluid model considers the dynamics of the separate phases rather than the mixture. Accordingly the model includes the six conservation equations for the mass, momentum and energy of each phase, generated by the averaging process described in Sect. 2.1. Jump conditions are posed at the interface (for example, the interfacial sources of gas and liquid must sum to zero). Drew and Wood [20] present a rigorous derivation of the two-fluid model, and discuss the many constitutive relations that must be prescribed in order to close the model. The two-fluid model is the most realistic of the three approaches discussed here,

particularly for flows such as annular flow where the velocities of the phases are quite different. Since we wish to model a length of boiling two-phase flow over which complete evaporation may take place, the model we present in Sect. 4 is essentially a two-fluid model.

3 Stability

The first successful analysis of unstable two-phase flow is widely acknowledged to be by Ledinegg [36], who studied the large scale flow excursions now referred to as Ledinegg instability. Ledinegg observed experimentally that the gradient of the steady state pressure drop-inlet flow curve $\Delta p(G)$ could become negative, depending on the operating conditions. In this case, a flow excursion to another steady state could occur. Ledinegg derived a cubic dependence for $\Delta p(G)$, based on simple correlations for the components of the pressure drop and assuming a uniform heat flux, and hence predicted when such instabilities occurred. The conditions giving rise to a negative slope of $\Delta p(G)$ were also investigated by Profos [38, 39] and Chilton [13]. Profos allowed for thermodynamic non-equilibrium (superheated liquid in the single and two-phase regions), and introduced a stability parameter equivalent to the nondimensional gradient $(G/\Delta p)\,\partial\Delta p/\partial G$; Chilton took the pressure drop as due only to friction, and considered nonuniform heat input profiles.

Quandt [40] recognised the two distinct types of two-phase flow instabilities, flow excursions and flow oscillations, and investigated the onset of oscillations both experimentally and theoretically. The analysis was based on a one-dimensional homogeneous model, consisting of equations of mass, momentum, energy and state for the mixture, in which small perturbations were applied to the dependent variables. In order to obtain an approximate solution, Quandt adopted a "lumping" technique to simplify the system, in which the perturbation to the flow rate was assumed to be linear in position and that of enthalpy was due to the integrated axial heat flux respectively. Integration along the channel and Laplace transformation then yielded a second-order characteristic equation for the response of the inlet flow to a perturbation in the heat flux. Oscillations were predicted for sufficiently low mass flow, depending on flow conditions. Quandt plotted the oscillation criteria on a Δp-G plane. Along the critical curve, Δp increases smoothly with increasing G, and oscillatory instabilities occur above the curve. The analytic criteria predicted flow oscillations at exit qualities lower than observed, the discrepancy increasing at higher operating pressures. This work was extended by Wallis and Heasley [47], who carried out a linear stability analysis of a homogeneous model posed in Lagrangian coordinates. Moreover, the "lumping" assumptions adopted by Quandt were relaxed. A complicated transfer function was derived, and stability was investigated by a Nyquist locus technique; however, no results were presented for the constant pressure drop case.

In the mid-sixties, the homogeneous model became formalised with the work of Bouré [8] and Davies and Potter [14]. Both studies were based on a one-dimensional homogeneous model, whose linear stability was examined in the standard manner of Laplace transformation and Nyquist analysis. Bouré set out to show that the "density effect" (the consequence of the variation of mixture density on

mixture enthalpy), and the consequent delay times in the system, were the sources of oscillatory instability. Both of these analyses were described at a timely symposium on two-phase flow dynamics held in Eindhoven [11, 14].

Another presentation at this symposium by Zuber [51] used an alternative modelling approach, the drift-flux theory developed by Zuber and Finlay [52], to investigate stability in the standard manner. A similar characteristic equation to the earlier homogeneous studies was obtained. Zuber and Staub [53, 54] used the drift-flux model to analyse kinematic waves in boiling two-phase flow, and derived a void propagation equation for constant and oscillatory flow and power conditions. Criteria for instability were finally presented by Ishii [31] who determined the stability boundary dividing stable and oscillatory unstable regions. Later Saha and Zuber [45] extended the analysis to include thermodynamic non-equilibrium effects.

Homogeneous models continued to be popular in the 1970s for the analysis of oscillatory instability. Yadigaroglu and Bergles [50] added the effects of wall thermodynamics, and the dependence of saturation enthalpy on pressure, and obtained a transfer function of inlet flow to pressure drop. The authors also carried out experiments and discovered transitions to higher mode oscillations for sufficiently large subcooling and low heating.

All of the studies on density-wave oscillations discussed so far consider linear stability of the steady state solutions. The first *nonlinear* analysis was given by Friedly and Krishnan [25], who used the Poincaré–Lindstedt method to analyse small steady oscillations. The analysis, based on a homogeneous model in which the pressure drop was solely due to inlet and outlet restrictions, was later extended by Krishnan et al. [35] to include the pressure drop components in the channel. Fowler [23] carried out a linear and nonlinear stability analysis of a homogeneous model which considered the pressure gradient due to wall shear only. In the nonlinear analysis, Fowler used the method of multiple scales to investigate the evolution of small oscillations to equilibrium limit cycles.

Studies of density-wave oscillation in the 1980s used a range of models and stability techniques. Achard et al. [1] investigated the linear stability of a homogeneous, thermal equilibrium model, focusing on four dimensionless parameters: subcooling, inlet velocity, friction coefficient and the Froude number. The results show wedges of oscillatory instability butting into the stable region at low values of the friction parameter. The authors later considered the nonlinear stability of the model using the Poincaré–Lindstedt method [2]. Rizwan-uddin and Dorning [41] computed the linear stability boundaries of a drift-flux model, and investigated nonlinear stability again using a Poincaré–Lindstedt analysis. In a later paper [42], the model was reduced to a homogeneous form by taking the drift velocity of the gas as zero. A stability map for the homogeneous model was presented, together with the results of a direct numerical solution.

Dykhuizen et al. [21] based their analysis on a two-fluid model, including the wall thermodynamics, regions of bubbly and annular flow, and entrainment. Linear stability was examined by first finite-differencing the model equations in space, to give a system of linear ordinary differential equations. The eigenvalues of

the system matrix were calculated and the stability margins compared to experimental results. Roy et al. [43] demonstrated the equivalence of this approach with the standard transfer function-based method. The system of ODEs was integrated by Dykhuizen et al. [22] and density-wave oscillations were computed in the linearly unstable region of parameter space.

3.1 Stability maps

The linear stability results described above are mostly given in terms of graphs which depict regions of stability or instability, usually as functions of certain dimensionless parameters. Model equations are discussed further in Sect. 4, but it is convenient at this point to identify two particular dimensionless parameters which are commonly used in stability maps. If the heat flux delivered to a flow channel is Q per unit length per unit time, u_0 is the inlet velocity to the pipe, and the inlet flow is subcooled by an enthalpy Δh_l below the saturation value, then the phase change number is

$$N_{pch} = \left(\frac{\rho_l - \rho_g}{\rho_g}\right) q, \quad q = \frac{Ql}{\rho_l A L u_0}, \tag{3.1}$$

where l is the heated tube length, A is the cross-sectional area, ρ_g, ρ_l are gas and liquid densities, and L is latent heat. The subcooling number is

$$N_{sub} = \left(\frac{\rho_l - \rho_g}{\rho_g}\right) \sigma, \quad \sigma = \frac{\Delta h_l}{L}, \tag{3.2}$$

and σ is a kind of inverse Stefan number.

Bouré and Mikaila [11] used a homogeneous model to investigate flow instability. They obtained the map shown in Fig. 2, in terms of dimensionless velocity v^* and enthalpy h^*, given by

$$v^* = (h_R/L) q^{-1}, \quad h^* = (h_R/L)^{-1} \sigma, \tag{3.3}$$

where h_R is a reference enthalpy.

Ishii and Zuber predicted stability boundaries with the use of a drift-flux model [31]. Their results are shown in Fig. 3, which shows that, for N_{sub} given, stability is lost as N_{pch} increases (v^* decreases) and oscillatory instability occurs, as in Bouré and Mikaila's results. However, the stability boundary does not meet the line $N_{sub} = 0$ ($h^* = 0$), implying stability for zero subcooling, and the results do not show a region of static instability.

The stability plane shown in Fig. 3 is attractive to use as the curves of constant exit quality (the mass fraction of steam at the exit) are parallel lines. One can show that the exit quality is

$$x_e = \frac{\rho_g}{\rho_l - \rho_g} (N_{pch} - N_{sub}) = q - \sigma, \tag{3.4}$$

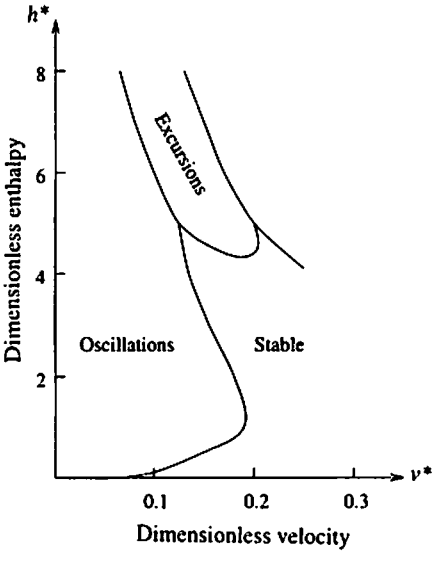

Fig. 2. Stability map of Bouré and Mikaila (from Ishii [31], p. 2.118)

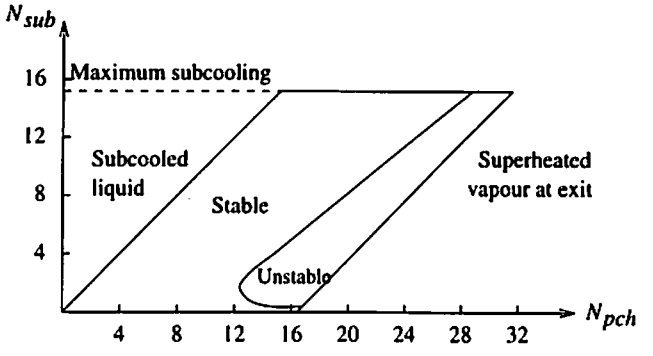

Fig. 3. Stability map of Ishii and Zuber (from Ishii [31], p. 2.119)

and Fig. 3 shows that the flow is stable for sufficiently low x_e. In fact, the simple stability criterion that the exit quality is below a critical value (calculated as a function of several operating parameters) has been suggested.

Ishii and Zuber's drift-flux approach was refined by Saha and Zuber to include thermal non-equilibrium. The results of both these analyses were compared with experimental data by Saha et al. [44]. Figure 4 shows the difference between the two analytically-derived stability boundaries and those found by experiment. The non-equilibrium theory appears to give better results for low N_{sub}, while for higher subcooling the results of the equilibrium theory are closer to the data.

Achard et al. [1] investigated stability boundaries using a homogeneous equilibrium model. Their approach included and emphasised the effects of varying

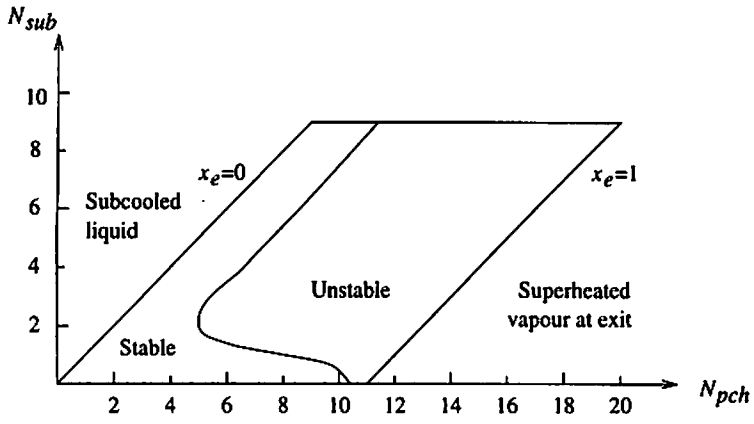

Fig. 4. Stability map of Saha et al. [44]

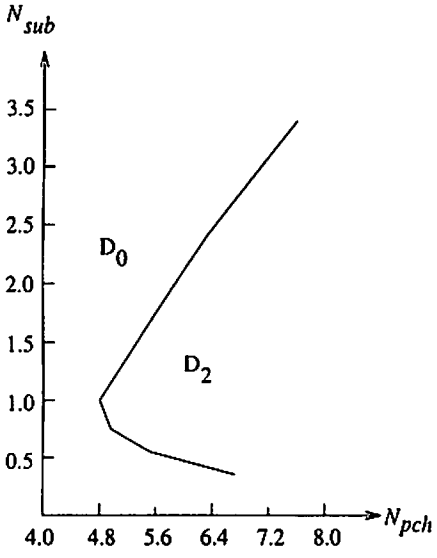

Fig. 5. Results of Achard et al. [1], showing marginal stability curves in the N_{sub}–N_{pch} plane, $Fr^{-1}=0$

a friction coefficient Λ and Froude number Fr. For the case $Fr^{-1} = 0$ (i.e., neglecting gravity) the stability boundary is similar to that of Ishii and Zuber (see [31]) and is shown in Fig. 5.

Figure 6 shows the stability map derived by Fowler [23] using a homogeneous, equilibrium model in which inertial (and gravitational) terms were neglected in the momentum equation. The coordinates of the map are τ_0 and $\lambda - \tau_0$, respectively, subcooling and exit quality. In terms of the parameters σ and q, $\tau_0 = \sigma$ and $\lambda = q$. The results again show a region of stability for low exit quality, which Fowler was in fact able to show using an expansion based on the dimensionless transit time in the two-phase region being small. The range of inlet subcooling (τ_0) includes

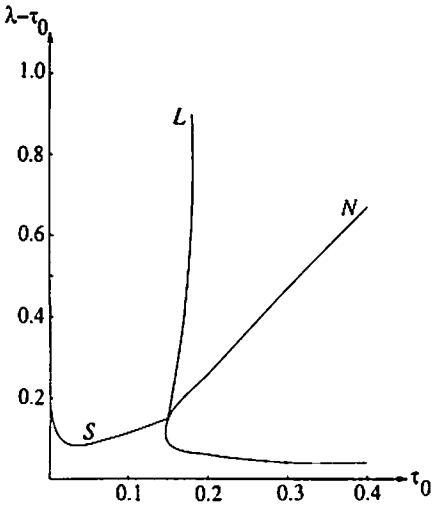

Fig. 6. Stability map of Fowler [23], showing three curves N, L, and S. N is the curve on which in the steady state $\partial\Delta p/\partial u_0 = 0$, and includes the unmarked lower branch. Ledinegg instability exists to the right of the curve L, whose lower branch coincides with that of N. To the left of L, oscillatory instability exists above the curve S; below S, the flow is stable

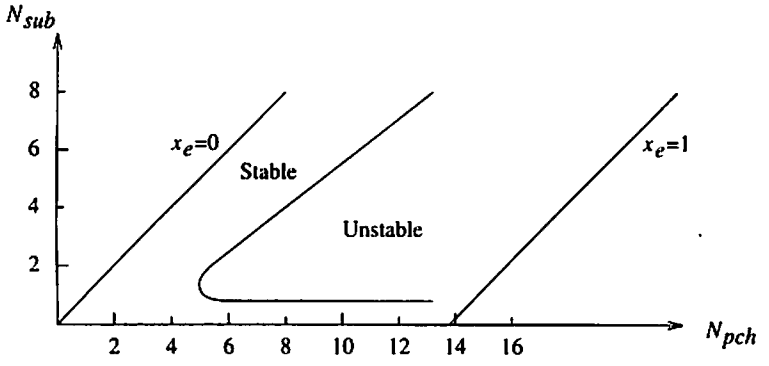

Fig. 7. Stability map of Dykhuizen et al. [21], showing boundary of oscillatory instability

a region of static instability at higher values of τ_0, as in Bouré and Mikaila's findings. A particular feature in Fig. 6 is the wedge of static instability between the upper branches of L and N, where $\partial\Delta p/\partial u_0 > 0$. Fowler thus claimed that the condition $\partial\Delta p/\partial u_0 < 0$ was not the necessary and sufficient condition for static (Ledinegg) instability as had been previously asserted, but that static instability could exist for positive values of $\partial\Delta p/\partial u_0$.

Most previous studies on stability boundaries have been based on homogeneous and drift-flux models. Dykhuizen et al. [21] used a two-fluid model, incorporating thermal non-equilibrium. Their results (Fig. 7) are very similar to those of Ishii and Zuber (see [31]) and Achard et al. [1], and again only show the boundary between regions of stability and oscillatory instability.

The most recent results we review are those of Rizwan-uddin and Dorning [42], who based their analysis on a drift-flux model. Figure 8 shows the stability map

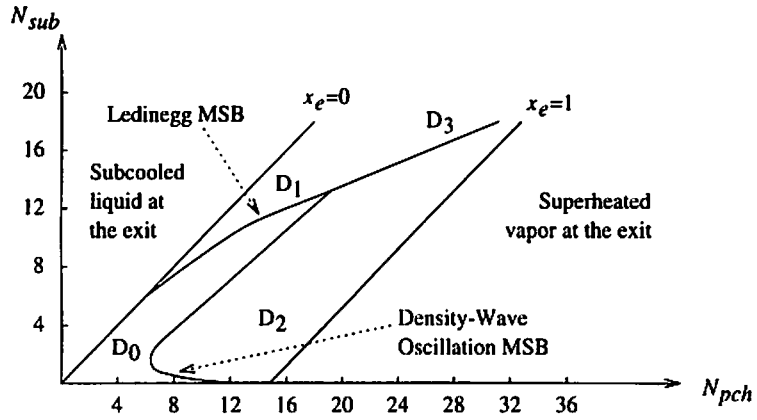

Fig. 8. Stability map of Rizwan-uddin and Dorning [42], showing analytically-derived boundaries of Ledinegg and oscillatory instability

they obtained; Ledinegg instability occurs for sufficiently high subcooling, even for low exit quality. However, the correspondence of the boundary of the D_1 region and a curve on which $\partial \Delta p / \partial u_0 = 0$ is not clear. The map is similar to that of Bouré and Mikaila [11] (though of course the latter authors use the coordinate $h^* \sim 1/N_{sub}$).

In order to compare the results reviewed so far (with each other and the results of the analysis presented in Sect. 4), it is beneficial to present them using a common coordinate system, as much as this is possible. The natural choice for the map coordinates would seem to be dimensionless subcooling and exit quality, which in terms of the parameters introduced in this analysis are σ and $x_e = q - \sigma$. Five of the seven reviewed studies adopt the subcooling and phase-change numbers N_{sub} and N_{pch} as coordinates; from (3.1) and (3.2) we see that we must rescale these values by the density ratio $\rho_g/(\rho_l - \rho_g)$. This ratio is unknown for the study of Achard et al. [1], hence we replot their results on a $(N_{sub}, N_{pch} - N_{sub})$ plane. Otherwise its value may be ascertained from the respective stability maps. The coordinates used by Bouré and Mikaila [11] are given by (3.3), but since the reference enthalpy h_R is unspecified, we display the results using new coordinates $(h^*, 1/v^* - h^*)$. Finally, the coordinates adopted by Fowler [23] are precisely those we have chosen above.

Figure 9 shows the redrawn stability planes. For each graph, a selection of points lying on the boundaries was replotted, the intention being to give a rough guide rather than a precise translation of the results. Several common features are apparent from Figs. 6 and 9. As the subcooling increases from zero, stability exists if the exit quality lies below a characteristically L-shaped curve; above this curve lies a region of oscillatory instability. For higher subcoolings, three of the maps show a wedge of Ledinegg instability displacing the stable region. Only Fowler [23] shows stability below this wedge (and both oscillatory and Ledinegg instability coexisting above it).

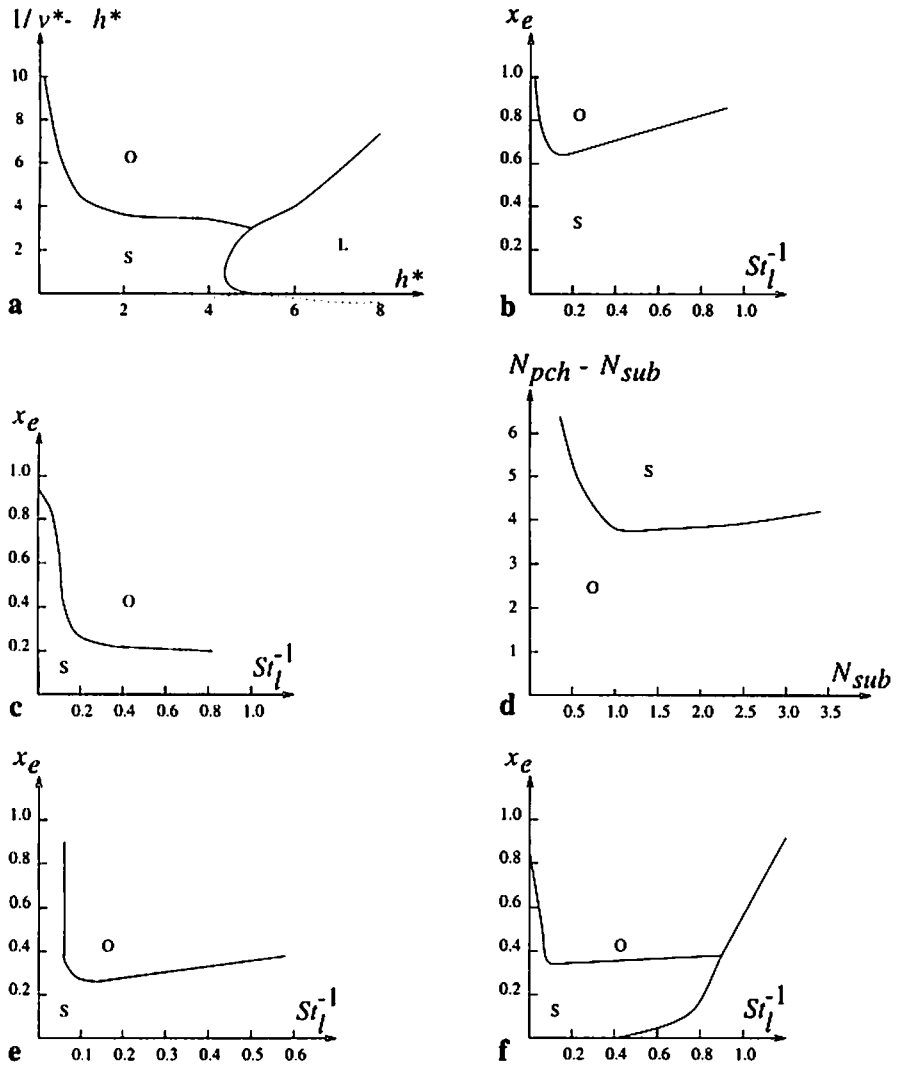

Fig. 9. Results of previous analyses replotted: a Bouré and Mikaila [11], b Ishii and Zuber [31], c Saha et al. [44], d Achard et al. [1], e Dykhuizen et al. [21], f Rizwan-uddin and Dorning [42]. *S*, *O*, and *L*, Regions of stability, and oscillatory and Ledinegg instability

3.2 Nonlinear stability

In order to investigate the amplitude of oscillations, a nonlinear stability analysis must be carried out. Most of the analytically-based studies presented in the literature [2, 25, 35, 41] have employed the Poincaré–Lindstedt method to investigate weakly nonlinear stability, while the method of multiple scales has also been used [23]. More recently, finite difference methods have been applied to solve numerically the model equations [22, 42]. Although the results of analytical

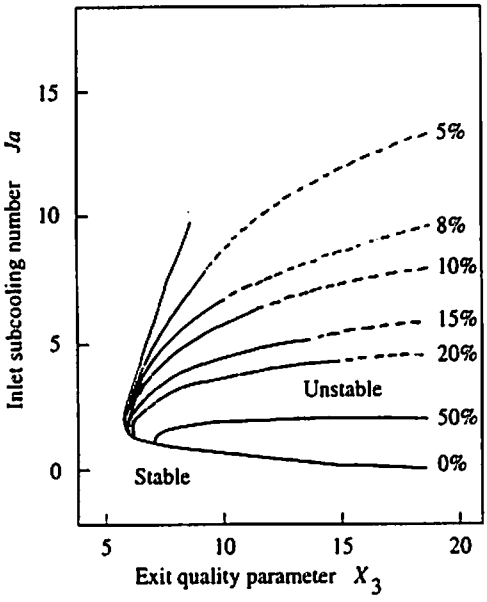

Fig. 10. Results of Krishnan et al. [35], showing contours of relative amplitude of inlet velocity oscillations. The labels on the curves express the equilibrium amplitude as a percentage of the steady state value. The dotted portions of the curves correspond to regions where the convergence of the perturbation series in the frequency is questionable, and hence results may be unreliable here

approaches are easier to generalise than numerically-based results, the algebra may become cumbersome as higher-order terms in the perturbation expansions are examined [35].

Friedly and Krishnan [25] based their pioneering analysis on a homogeneous equilibrium model, in which the pressure drop was entirely due to flow restrictions at the inlet and outlet. Their work was later continued by Krishnan et al. [35] to include the components of the pressure drop in the channel. The Poincaré–Lindstedt method, used in both these studies, essentially determines the nonlinear modifications of amplitude and frequency of oscillating solutions for a point in the neighbourhood of the marginal stability boundary (MSB), to those of a linearised solution for a point on the MSB, via asymptotic expansion and matching techniques. This method was employed to compute to a first approximation the amplitude of oscillations as system parameters were varied. In particular, Krishnan et al. used the parameters Ja (Jakob number) and X_3, representing the subcooling and exit quality respectively, and varied the relative pressure drop components. The amplitude of the oscillations of the inlet velocity was calculated, and results were shown as contours of the ratio of the amplitude to the associated steady state value. Figure 10 shows the curves plotted on the X_3-Ja plane, for the case when the dominant pressure drop component is due to channel friction.

A supercritical Hopf bifurcation occurs at the MSB: moving from the stable into the unstable region of parameter space, the amplitude of oscillation increases with the square root of the distance from the neutral stability curve. On the lower branch of the MSB (labelled "0%"), a small increase in Ja leads to a very large increase in the amplitude, and it was suggested that this result is the same as the "burst" in the amplitude discovered by Fowler [23], though as we describe below,

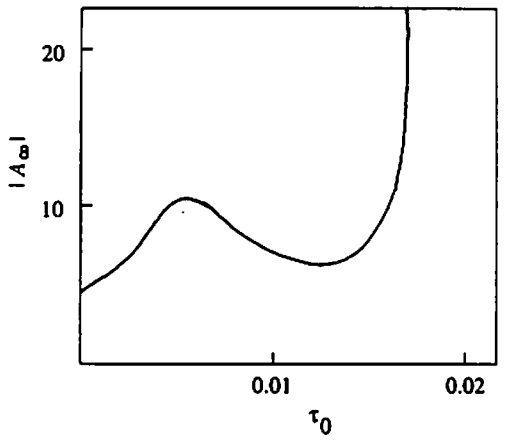

Fig. 11. Results of Fowler [23], showing the measure of the growth of inlet velocity oscillations at the marginal stability boundary $|A_\infty|$ vs. dimensionless subcooling τ_0

this occurred for subcoolings above a small value. Krishnan et al. compared their calculations with results from experiments; though the orders of magnitude are similar, there is little qualitative agreement. The authors point out that there are few systematic experimental data to guide analytical investigations of flow oscillations.

Fowler [23] investigated the weakly nonlinear stability of a homogeneous model, taking the pressure drop as entirely due to channel friction. This analysis used the method of multiple scales, in which the amplitude of the small oscillations is time-dependent (rather than constant as in Poincaré's method). A supercritical Hopf bifurcation occurs at the MSB (the curve labelled "S" in Fig. 6). A measure of the growth of the amplitude on the unstable side of the MSB was calculated and is shown in Fig. 11. Increasing the subcooling $\tau_0 = \sigma$ from zero, we see $|A_\infty|$ initially reaches a maximum and a minimum before increasing unboundedly at $\tau_0 \approx 0.02$. The asymptotic analysis breaks down in this case, and Fowler suggested that this "burst" corresponded to earlier experimental observations of rapidly increasing amplitudes [33].

Achard et al. [2] used the Poincaré–Lindstedt method to analyse the nonlinear stability of a homogeneous model. Results were shown as contours of ε, the measure of the amplitude on which the series expansions are based, on a plane with dimensionless coordinates subcooling number N_{sub} and friction number Λ; Fig. 12 gives an example. For sufficiently large Λ, the positive contours lie in the unstable region, and the Hopf bifurcation is supercritical; otherwise the finite-amplitude oscillations are found on the stable side of the MSB, corresponding to a subcritical Hopf bifurcation. Achard et al. point out that the contours may be interpreted in terms of the allowable noise in the system. In addition, the MSB gives a good representation of the operational stability boundary observed in practice, when the contours lie in close proximity to it.

Dykhuizen et al. [22] calculated the numerical solution for a (relatively complicated) two-fluid model, which included wall thermodynamics, subcooled boiling, bubbly and annular regimes and entrainment. The model was first finite differenced

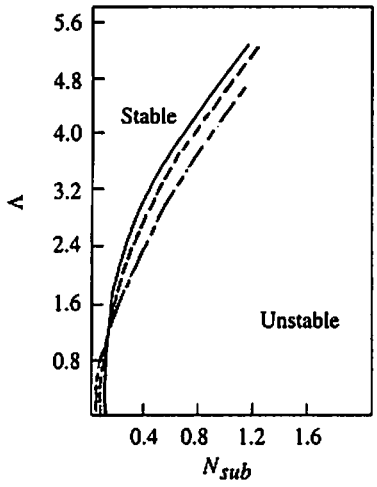

Fig. 12. Results of Achard et al. [2], showing contours of ε, a measure of the amplitude of oscillations. The solid curve is the MSB ($\varepsilon = 0$), the adjacent regular-dashed curve corresponds to $\varepsilon = 0.3$, and the long-short-dashed curve to $\varepsilon = 0.5$

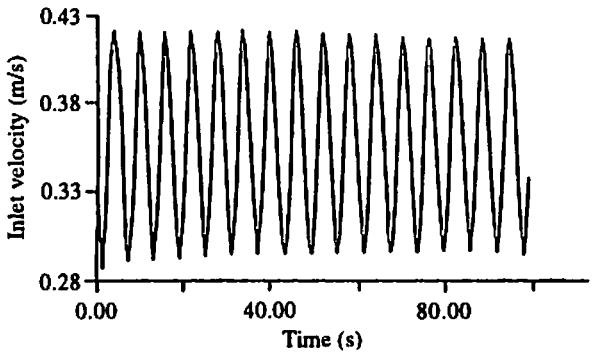

Fig. 13. Results of Dykhuizen et al. [22], showing density-wave oscillations after initial perturbations to the heating power. In this case, the power is varied linearly from 92 to 97 to 94 kW in the first two seconds

in space to yield a system of first-order ODEs. The discretisation is time-dependent, as the cell boundaries are allowed to move in accordance with the moving boundaries (which demarcate the single-phase and two-phase regions). The ODEs were integrated with a fully implicit method, using a package designed for stiff systems. In order to investigate the amplitude of oscillations, the system was initially set at an unstable steady state, and one or two large perturbations imposed on the heat input. This approach led to limit cycles being reached relatively quickly, and was motivated by the computational expense of continuing calculations over long times, and similar experimental procedures. Figure 13 shows an example of the inlet velocity history.

A drift-flux model was analysed by Rizwan-uddin and Dorning [41] using the Poincaré–Lindstedt method. As before, supercritical Hopf bifurcation was identified at the MSB. In a later paper [42], the authors adopted a simpler homogeneous

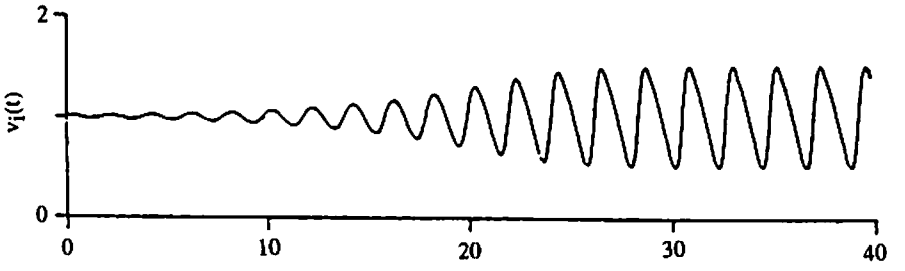

Fig. 14. Results of Rizwan-uddin and Dorning [42], showing the inlet velocity v_i vs. time for parameters on the edge of the unstable region, following a perturbation to v_i at $t = 0$

model, which is integrated to yield a nonlinear, variable-delay, integro-differential equation for the inlet velocity. The solution was obtained numerically using a fully implicit method, for cases of constant, exponentially decaying and oscillatory pressure drop. In the former case, supercritical Hopf bifurcation was again demonstrated. The inlet velocity response to an initial perturbation was presented for a sequence of points crossing the MSB: Fig. 14 shows an example of the results computed on the edge of the unstable region. With an oscillatory pressure drop boundary condition, a chaotic response was possible.

4 A reduced model

It is possible to derive a relatively simple two-fluid model from some of the very complicated averaged models proposed by Drew and Wood [20], for example. This is in fact done by Aldridge [3], but for brevity here we only sketch the procedure.

Let us suppose subcooled water is forced through a pipe $0 < z < l$ by a pressure drop Δp, subject to a heat input Q per unit length per unit time. We suppose as is usual that the flow is turbulent, and that the model equations are cross-sectionally averaged. We will further suppose that boiling occurs at $z = r(t)$, where the temperature reaches the saturation value, and that the remainder of the tube $r(t) < z < l$ is two-phase, that is dryout does not occur. (For example, this is the situation we wish to study in nuclear reactor coolant tubes.)

4.1 Single-phase region

If the water is taken as incompressible, then in $z < r(t)$, the liquid velocity is $u_l = u_0(t)$, where u_0 is the inlet velocity, and then momentum and enthalpy equations can be written as

$$\begin{aligned} \rho_l u_{0t} &= -p_z + F_{lw} + \rho_l g_a, \\ \rho_l [h_{lt} + u_0 h_{lz}] &= Q/A, \end{aligned} \tag{4.1}$$

where ρ_l is the liquid density, p is the pressure, F_{lw} is a two-phase turbulent frictional term, g_a is the axial component of gravitational acceleration, h_l is the

liquid enthalpy, and A is the cross-sectional area. Subscripts l and w denote liquid and wall (and later g is for gas, i is for interface) but t and z subscripts denote partial derivatives. If h_l is prescribed to be h_{l0} at $z = 0$, then the solution of $(4.1)_2$ is just (if Q is constant)

$$z = \int_{t - \rho_l A(h_l - h_{l0})/Q}^{t} u_0(s)\,\mathrm{d}s, \tag{4.2}$$

and in particular, the boiling boundary is given by

$$r(t) = \int_{t-\tau_0}^{t} u_0(s)\,\mathrm{d}s, \tag{4.3}$$

where the delay is

$$\tau_0 = \frac{\rho_l A \Delta h_l}{Q} \tag{4.4}$$

and Δh_l is the inlet enthalpy subcooling, $h_l^{\mathrm{sat}} - h_{l0}$, where h_l^{sat} is the saturation value.

The momentum equation is simply used as a quadrature to compute the single-phase pressure drop. For example, a typical correlation for F_{lw} is

$$F_{lw} = -\frac{2}{d} f_{lw} \rho_l u_l |u_l|, \tag{4.5}$$

where d is tube diameter, and f_{lw} is a friction factor of typical size 0.005 which itself depends weakly on a Reynolds number (and hence on u_l). At any rate, the single-phase pressure drop is given in terms of the unknown $u_0(t)$ by

$$\Delta p_{sp} = (-F_{lw} - \rho_l g_a + \rho_l u_{0t}) r. \tag{4.6}$$

4.2 Two-phase flow region

A two-fluid model for the two-phase flow region consists of six conservation equations, two each of mass, momentum and energy (or enthalpy) for each phase, together with three interfacially averaged jump conditions representing total interfacial sources of mass and momentum (both zero) and enthalpy (non-zero because of latent heat). We give these in detail here to illustrate the complexity of the two-fluid models, although we later simplify them dramatically. The six conservation laws are

$$\begin{aligned}
(\alpha\rho_g)_t + (\alpha\rho_g v)_z &= \Gamma_g, \\
(\beta\rho_l)_t + (\beta\rho_l u)_z &= \Gamma_l, \\
(\alpha\rho_g v)_t + (C_{vg}\alpha\rho_g v^2)_z &= -[\alpha(p_g + p_g^{Re} - \tau_g)]_z + p_{gi}\alpha_z \\
&\quad + F_{gi} + F_{gw} + v_{gi}\Gamma_g + \alpha\rho_g g_a, \\
(\beta\rho_l u)_t + (C_{vl}\beta\rho_l u^2)_z &= -[\beta(p_l + p_l^{Re} - \tau_l)]_z + p_{li}\beta_z \\
&\quad + F_{li} + F_{lw} + v_{li}\Gamma_l + \beta\rho_l g_a,
\end{aligned} \tag{4.7}$$

$$(\alpha\rho_g h_g)_t + (C_{hg}\alpha\rho_g v h_g)_z = -[\alpha(q_g + q_g^{Re})]_z + \frac{\xi}{A} q_{gw}\alpha_w + E_g + h_{gi}\Gamma_g + \alpha\tau_g v_z + \alpha D_g + \hat{P}_g + \alpha(p_{gt} + v p_{gz}),$$

$$(\beta\rho_l h_l)_t + (C_{hl}\beta\rho_l u h_l)_z = -[\beta(q_l + q_l^{Re})]_z + \frac{\xi}{A} q_{lw}\beta_w + E_l + h_{li}\Gamma_l + \beta\tau_l u_z + \beta D_l + \hat{P}_l + \beta(p_{lt} + u p_{lz}),$$

wherein α and β are the volume fractions for gas and liquid respectively (thus $\alpha + \beta = 1$), v and u are their respective velocities, h_g and h_l the enthalpies. Other terms are the mass sources Γ_k, the profile parameters C_{hk}, C_{rk} (representing effects of the averaging), the Reynolds stresses p_k^{Re}, the shear stresses τ_k, the interfacial pressures p_{ki}, interfacial and wall shear stresses F_{ki}, F_{kw}, interfacial average velocities v_{ki}, axial, turbulent, and wall heat fluxes q_k, q_k^{Re}, q_{kw}, interfacial enthalpies h_{ki}, interfacial heat sources E_k, viscous dissipation terms D_k, and pressure work terms $\hat{P}_k$; ξ is the tube perimeter.

In addition, we have the three interfacial jump conditions

$$\begin{aligned} \Gamma_g + \Gamma_l &= 0, \\ p_{gi}\alpha_z + F_{gi} + p_{li}\beta_z + F_{li} + v_{gi}\Gamma_g + v_{li}\Gamma_l &= 0, \\ E_g + E_l + h_{gi}\Gamma_g + h_{li}\Gamma_l &= 0. \end{aligned} \tag{4.8}$$

It is possible to nondimensionalise these equations and demonstrate that many of the terms are in fact negligible, and this is done by Aldridge [3]. Here we take a short cut along the same route. It may be shown that in normal operating conditions, the liquid and gas enthalpies are almost in equilibrium at their saturation values. (This cannot be exactly true, for example, in annular flow, where the liquid must be superheated in order that evaporation occurs at the gas–liquid interface.) It then follows that all the heat input in the two-phase region is absorbed as latent heat, whence it follows that

$$\Gamma_g = \Gamma = \frac{Q}{AL}, \tag{4.9}$$

where L is the latent heat, defined as $h_g^{sat} - h_l^{sat}$.

The two conservation of mass equations are thus (with ρ_l constant)

$$\begin{aligned} \rho_l[\beta_t + (\beta u)_z] &= -\Gamma, \\ (\alpha\rho_g)_t + (\alpha\rho_g v)_z &= \Gamma. \end{aligned} \tag{4.10}$$

In approximating the gas momentum equation, it is found that the dominant terms are simply

$$\alpha p_z = F_{gi}, \tag{4.11}$$

where we have used interfacial constitutive laws that imply $p_g \approx p_{gi} (\approx p_{li} \approx p_l)$. The neglect of the acceleration terms is a singular approximation which has the

effect of filtering acoustic waves associated with gas compressibility. It is safe to lose these terms provided we let acoustic waves go. A similar argument for the liquid momentum equation allows its reduction to

$$\beta p_z = -F_{gi} + F_{lw}, \tag{4.12}$$

where the interfacial momentum transfer ((4.8), second condition) is essentially a force balance $F_{gi} = -F_{li}$.

4.3 Nondimensionalisation

In order to understand the structure of the equations, we must give constitutive relations for F_{gi} and F_{lw}. We use the same expression for F_{lw} as before,

$$F_{lw} = -\frac{2}{d} f_{lw} \rho_l u |u|, \tag{4.13}$$

with f_{lw} depending weakly on u (and also β). A similar expression for F_{gi} can be written, viz,

$$F_{gi} = -\frac{2 f_{gi}}{d} \rho_g (v - u)|v - u|, \tag{4.14}$$

where f_{gi} is a complicated function of α, u, and v which depends on the flow regime in question.

The reduced two-fluid model given by (4.10), (4.11), and (4.12) is very close to that derived by Seward [46] for annular flow in different operating conditions. To see the structure of these equations, observe that

$$\begin{aligned} F_{gi} &= \alpha F_{lw}, \\ p_z &= F_{lw}. \end{aligned} \tag{4.15}$$

The second of these, as a quadrature will give the two-phase pressure drop Δp_{tp} as a function of $u_0(t)$. Hence the total pressure gradient $\Delta p = \Delta p_{sp} + \Delta p_{tp}$ is given as a function of $u_0(t)$, and is equal to the prescribed value, thus providing an equation for u_0. If, for example, ρ_g, f_{gi} and f_{lw} are constants, then $(4.15)_1$ gives $v \propto u$, and (4.10) consists of two hyperbolic equations for β and u, with conditions of continuity of both at $z = r$; thus

$$\beta = 1, \quad u = u_0 \quad \text{at } z = r. \tag{4.16}$$

In order to nondimensionalise the equations, we choose scales for the variables ρ_g, r, u, v, t, z, Δp, u_0, Γ as follows (α, β are unscaled):

$$\begin{aligned} \rho_g &\sim \bar{\rho}_g \\ r &\sim z \sim l, \\ t &\sim l/u, \\ \frac{\Delta p}{l} &\sim \frac{2}{d} \bar{f}_{lw} \rho_l u^2, \\ \rho_g v &\sim \rho_l u_0 \sim \Gamma l. \end{aligned} \tag{4.17}$$

Here $\rho_g, \bar{f}_{lw}$ and $\bar{f}_{gi}$ are typical values of ρ_g, f_{lw} and f_{gi}. The inlet velocity is scaled by a typical value, which is distinct from the liquid velocity scale, since in the two-phase region, particularly in annular flow, the liquid can be rapidly accelerated.

The velocity scales determined from (4.17) are thus

$$u \sim U = \left(\frac{d\Delta p}{2\bar{f}_{lw}\rho_l l}\right)^{1/2}, \quad v \sim V = \frac{\rho_l U_0}{\bar{\rho}_g}, \tag{4.18}$$

where $u_0 \sim U_0$, and the corresponding dimensionless equations (4.3) and (4.6) are

$$\begin{aligned} r &= \delta \int_{t-\tau_0}^{t} u_0(s)\,ds, \\ \Delta p_{sp} &= f_{lw}^* r u_0^2, \end{aligned} \tag{4.19}$$

in the single-phase region, where we neglect gravity and inertia as being small (they are easily included, though). The parameters are

$$\delta = \frac{U_0}{U}, \quad \tau_0 = \frac{\rho_l A U \Delta h_l}{Ql} = \frac{\sigma}{\gamma\delta}, \tag{4.20}$$

in terms of σ and γ defined by

$$\sigma = \frac{\Delta h_l}{L}, \quad \gamma = \frac{Ql}{\rho_l A L U_0}, \tag{4.21}$$

so σ and $q = \gamma/u_0$ are as defined earlier by (3.1) and (3.2). In dimensionless form, the two-phase flow equations (4.10) and (4.15) are (with $\alpha + \beta = 1$)

$$\begin{aligned} \lambda(\alpha\rho_g)_t + (\alpha\rho_g v)_z &= \gamma, \\ \beta_t + (\beta u)_z &= -\delta\gamma, \\ f_{gi}^* \rho_g (v - \lambda u)^2 &= \mu\alpha f_{lw}^* u^2, \\ \Delta p_{tp} &= \int_r^1 f_{lw}^* u^2\,dz, \end{aligned} \tag{4.22}$$

where

$$\lambda = U/V, \quad \mu = \frac{dP}{2l\bar{f}_{gi}\bar{\rho}_g V^2}, \tag{4.23}$$

and we prescribe continuity of β and u at $z = r$, i.e.,

$$\beta = 1, \quad u = \delta \quad \text{on } z = r. \tag{4.24}$$

In these equations, realistic correlations would give the $O(1)$ friction number f_{lw}^* as a weak function of u_0 in (4.19), and as a function of β and u in (4.22), while f_{gi}^* may be taken as a function of α (or β), u, and v. We implicitly assume $v > \lambda u > 0$ in writing the quadratic friction terms.

Typical values of the input parameters are taken as the following:

$$\begin{gathered}\bar{\rho}_g = 32\ \text{kg/m}^3,\ \rho_l = 760\ \text{kg/m}^3,\ d = 0.016\ \text{m},\ l = 20\ \text{m},\\ U_0 = 1.3\ \text{m/s},\ \Delta p = 10\ \text{bars},\ \bar{f}_{lw} = 2.1\times 10^{-3},\ \bar{f}_{gi} = 0.2,\\ A = 2\times 10^{-4}\ \text{m}^2,\ \Delta h_l = 1.2\times 10^6\ \text{J/kg},\ Q = 1.6\times 10^4\ \text{W/m},\\ L = 1.6\times 10^6\ \text{J/kg},\end{gathered} \tag{4.25}$$

and from these we derive the velocity scales

$$U \sim 16\ \text{m/s},\quad V \sim 31\ \text{m/s}, \tag{4.26}$$

and thus

$$\begin{gathered}\delta \approx 0.081,\quad \sigma \approx 0.75,\\ \gamma \approx 1.0,\ \lambda \approx 0.52,\ \mu \approx 0.065.\end{gathered} \tag{4.27}$$

We thus see that typically $\sigma, \gamma \sim O(1)$, while δ is small, which may lend itself to further approximations: we do not pursue such matters here.

5 Stability analysis

The reduced model derived in Sect. 4 can be analysed in a similar way to other models discussed previously. When realistic correlations for f_{lw} and f_{li} are used, much of the labour is numerical, but the asymptotic reduction of the model allows a relatively easy comparison with results from a direct simulation.

5.1 Steady states

Figure 15 shows dimensionless pressure drop versus scaled inlet velocity for a range of values of γ, at a fixed value of the subcooling $\sigma = 0.77$, and with other parameters as in (4.27). These are dimensionless values, using the scales indicated in (4.25) and (4.26). For increasing heating rates, we see the occurrence of multiple steady states (for prescribed Δp) associated with Ledinegg instability. The existence of these multiple steady states is associated with the fact that when γ is low (or u_0 is high), and the flow is entirely subcooled, then $\Delta p \sim \rho_l u_0^2$, whereas at high γ (low u_0), the flow is superheated steam, so that $\Delta p \sim \rho_g v^2$, and with $\rho_g v \sim \rho_l u_0$, then $\Delta p \sim (\rho_l/\rho_g)\rho_l u_0^2$. As u_0 increases, there is therefore a transition from large $\Delta p/\rho_l u_0^2$ to small $\Delta p/\rho_l u_0^2$.

5.2 Linear stability

By direct linearisation, we can study the parametric dependence of stability of the steady state on the two principal parameters q ($\sim N_{pch}$) and σ ($\sim N_{sub}$) and these

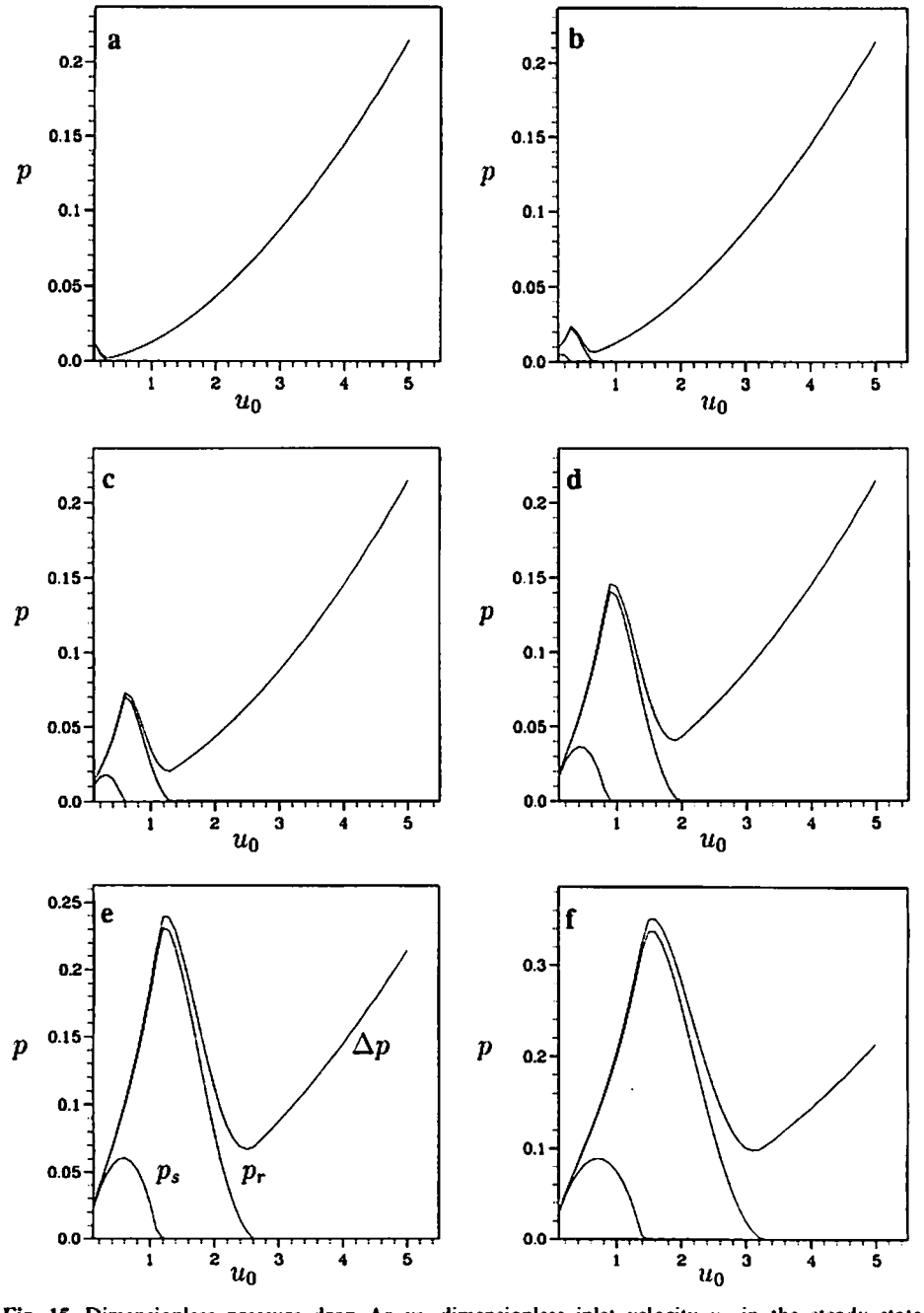

Fig. 15. Dimensionless pressure drop Δp vs. dimensionless inlet velocity u_0 in the steady state, with $\sigma = 0.77$ and a range of values of γ, from Aldridge [3]. The upper curve in each graph is the total pressure drop. The model used here included a region of superheated steam following dryout of the liquid phase at $z = s$, say; the middle and lower curves show the pressures at $z = r$ and $z = s$, respectively (taking dimensionless pressure as zero at the outlet). Values of γ: a 0.2, b 0.5, c 1.0, d 1.5, e 2.0, f 2.5

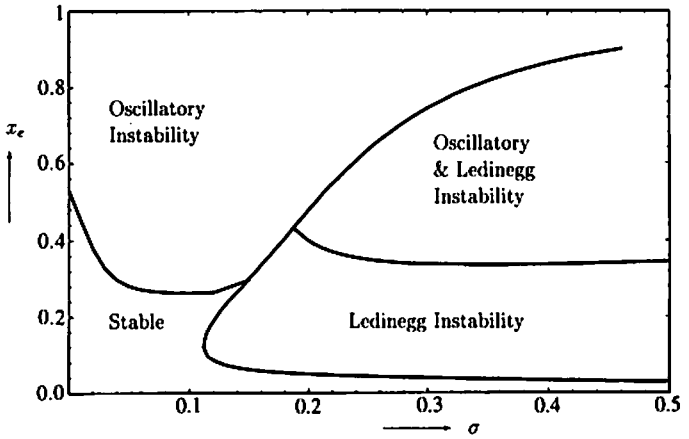

Fig. 16. Linear stability results from Aldridge [3], showing regions of Ledinegg and oscillatory instability, with $\gamma = 1$

can be compared to previous results. The results of this are shown in Fig. 16, where the parameters are exit quality $x_e = q - \sigma \propto N_{pch} - N_{sub}$, and subcooling $\sigma \propto N_{sub}$. This can be compared directly to the graphs in Sect. 3, and displays similar characteristics. At high inlet subcoolings, all flows with significant boiling (and hence exit quality) exhibit multiple steady states, and of the three possibly steady states, only the high flow (low x_e) one is stable. Practically, therefore, such high inlet subcoolings tend towards instability. At low subcoolings, hysteresis is not a problem, but the higher exit quality states are again unstable, this time to oscillatory states.

5.3 Nonlinear stability

We have verified the linear stability results by solving numerically the reduced model directly. In addition, we have used the code to study finite amplitude oscillations, and in particular, whether the Hopf bifurcation at low inlet subcoolings is subcritical or supercritical. We find that the bifurcation is everywhere supercritical along the marginal stability curve, and has an amplitude A (in inlet velocity) related to the degree of supercriticality by

$$A \approx c(x_e - x_e^*)^{1/2}, \tag{5.1}$$

where x_e^* is the value of exit quality on the critical curve (for $\sigma \lesssim 0.14$). The value of c is plotted in Fig. 17 as a function of subcooling σ. We see that c varies between 10 and 30, which suggests that, although the bifurcation is "soft", the resultant amplitudes quickly become significant (and therefore practically untolerable).

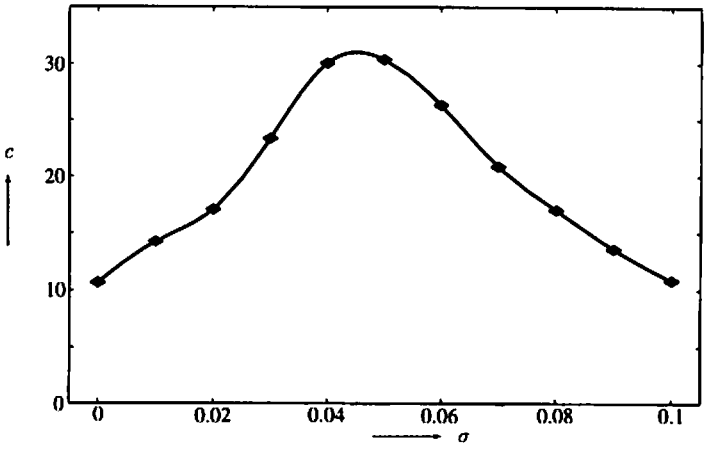

Fig. 17. Amplitude coefficient c in Eq. (5.1), calculated for $\sigma = 0.00, 0.01, \ldots, 0.10$, from Aldridge [3]

6 Conclusions

A survey of analytical and experimental results for heated steam-water flows reveals a broad consensus in the general results. We have indicated how an analysis of an asymptotically reduced model can be used to provide an easier comparison between linear stability results and direct numerical simulation. Our results also show how two-fluid models can be made analytically (and numerically) more tractable, and by the process of identifying explicitly the nondimensional parameters, we would be able in any given flow situation, to explicitly identify which terms are important. Further details of this procedure and the results will be published elsewhere.

Acknowledgement

The first author was supported by an SERC Research Studentship.

References

1. Achard, J.L., Drew, D.A., Lahey, R.T.: The effect of gravity and friction on the stability of boiling flow in a channel. AIChE Symp. Ser. 199, 76: 104–115 (1980).
2. Achard, J.L., Drew, D.A., Lahey, R.T.: The analysis of nonlinear density-wave oscillations in boiling channels. J. Fluid Mech. 155: 213–232 (1985).
3. Aldridge, C.J.: Density-wave oscillations in two-phase flows. D.Ph. thesis, University of Oxford, Oxford, U.K. (1995).
4. Anderson, T.B., Jackson, R.: A fluid mechanical description of fluidised beds. Ind. Eng. Chem. Fundam. 6: 527–539 (1967).
5. Bailey, N.A.: Introduction to hydrodynamic instability. In: Butterworth D., Hewitt, G.F. (eds.): Two-phase flow and heat transfer. Oxford University Press, Oxford, pp. 343–373 (1977).
6. Batchelor, G.K.: The stress system in a suspension of force-free particles. J. Fluid Mech. 41: 545–570 (1970).
7. Bergles, A.E.: Instabilities in two-phase systems. In: Bergles, A.E., Collier, J.E., Delhaye, J.M., Hewitt, G.F., Mayinger, F. (eds.): Two-phase flow and heat transfer in the power and process industries. Hemisphere, Washington, pp. 383–423 (1981).

8. Bouré, J.: The oscillatory behavior of heated channels. An analysis of the density effect. Part I: the mechanism (nonlinear analysis). Centre d'Etudes Nucléaires de Grenoble, Report CEA-R 3049 (1966).
9. Bouré, J.A., Bergles, A.E., Tong, L.S.: Review of two-phase flow instability. Nucl. Eng. Des. 25: 165–192 (1973).
10. Bouré, J.A., Delhaye, J.M.: General equations and two-phase flow modelling. In: Hetsroni, G. (ed.): Handbook of multiphase systems. Hemisphere, Washington, pp. 1.36–1.95 (1982).
11. Bouré, J., Mikaila, A.: The oscillatory behaviour of heated channels. In: Proceedings of the symposium on two-phase flow dynamics, Eindhoven, EUR 4288e, pp. 695–720 (1967).
12. Buyevich, Yu.A., Shchelchkova, I.N.: Flow of dense suspensions. Prog. Aerospace Sci. 18: 121–150 (1978).
13. Chilton, H.: A theoretical study of stability in water flow through heated passages. J. Nucl. Energy 5: 273–284 (1957).
14. Davies, A.L., Potter, R.: Hydraulic stability: an analysis of the causes of unstable flow in parallel channels. In: Proceedings of the symposium on two-phase flow dynamics, Eindhoven, EUR 4288e, pp. 1225–1266 (1967).
15. Delhaye, J.M.: Two-phase flow patterns. In: Bergles, A.E., Collier, J.E., Delhaye, J.M., Hewitt, G.F., Mayinger, F. (eds.): Two-phase flow and heat transfer in the power and process industries. Hemisphere, Washington, pp. 1–39 (1981).
16. Delhaye, J.M.: Basic equations for two-phase flow modelling. In: Bergles, A.E., Collier, J.E., Delhaye, J.M., Hewitt, G.F., Mayinger, F. (eds.): Two-phase flow and heat transfer in the power and process industries. Hemisphere, Washington, pp. 40–97 (1981).
17. Drew, D.A.: Averaged field equations for two-phase media. Stud. Appl. Math. 50: 133–166 (1971).
18. Drew, D.A.: Mathematical modelling of two-phase flow. Annu. Rev. Fluid Mech. 15: 261–291 (1983).
19. Drew, D.A., Lahey, R.T.: Application of general constitutive principles to the derivation of multidimensional two-phase flow equtions. Int. J. Multiphase Flow 5: 243–264 (1979).
20. Drew, D.A., Wood, R.T.: Overview and taxonomy of models and methods for workshop on two-phase flow fundamentals. National Bureau of Standards, Gaithersburg, MD (1985).
21. Dykhuizen, R.C., Roy, R.P., Kalra, S.P.: A linear time-domain two-fluid model analysis of dynamic instability in boiling flow systems. J. Heat Transfer 108: 100–108 (1986).
22. Dykhuizen, R.C., Roy, R.P., Kalra, S.P.: Two-fluid model simulation of density-wave oscillations in a boiling flow system. Nucl. Sci. Eng. 94: 167–179 (1986).
23. Fowler, A.C.: Linear and nonlinear stability of heat exchangers. J. Inst. Math. Appl. 22: 361–382 (1978).
24. Frankl, F.I.: On the theory of motion of suspended sediments. Dokl. Akad. Nauk SSSR 92: 247–250 (in Russian) (1953).
25. Friedly, J.C., Krishnan, V.S.: Prediction of nonlinear flow oscillations in boiling channels. AIChE Symp. Ser. 118, 68: 127–135 (1972).
26. Hassanizadeh, M., Gray, W.G.: General conservation equations for multiphase systems: 1. Averaging procedure. Adv. Water Resources 2: 131–144 (1979).
27. Hewitt, G.F.: Flow patterns. In: Butterworth, D., Hewitt, G.F. (eds.): Two-phase flow and heat transfer. Oxford University Press, Oxford, pp. 18–39 (1977).
28. Hewitt, G.F.: Flow regimes. In: Hetsroni, G. (ed.): Handbook of multiphase systems. Hemisphere, Washington, pp. 2.3–2.43 (1982).
29. Hinze, J.O.: Turbulence. McGraw-Hill, New York (1959).
30. Ishii, M.: Thermo-fluid dynamic theory of two-phase flow. Collection de la Direction des Etudes et Recherches d'Electricite de France. Eyrolles, Paris (1975).
31. Ishii, M.: Wave phenomena and two-phase flow instabilities. In: Hetsroni, G. (ed.): Handbook of multiphase systems. Hemisphere, Washington, pp. 2.95–2.122 (1982).
32. Ishii, M., Kocamustafaogullari, G.: Two-phase flow models and their limitations. In: Kakac, S., Ishii, M. (eds.): Advances in two-phase flow and heat transfer, vol. I. Martinus Nijhoff, The Hague, pp. 1–14 (NATO ASI series, series E, no. 63) (1983).
33. Jain, K.C.: Self sustained hydrodynamic oscillations in a natural circulation two-phase flow boiling loop. Argonne National Laboratory Report ANL-7073 (1965).
34. Kakac, S., Veziroglu, T.N.: A review of two-phase flow instabilities. In: Kakac, S., Ishii, M. (eds.): Advances in two-phase flow and heat transfer, vol. II. Martinus Nijhoff, The Hague, pp. 557–667 (NATO ASI series, series E, no. 64) (1983).
35. Krishnan, V.S., Atkinson, M.J., Friedly, J.C.: Nonlinear flow oscillations in boiling channels. AIChE Symp. Ser. 199, 76: 359–372 (1980).

36. Ledinegg, M.: Instability of flow during natural and forced circulation. Wärme 61: 891–898 (1938).
37. Nigmatulin, R.I.: Spatial averaging in the mechanics of heterogeneous and dispersed systems. Int. J. Multiphase Flow 5: 353–385 (1979).
38. Profos, P.: Stability of water distribution in forced-circulation heating surfaces. Sulzer Tech. Rev. 1: 1–8 (1947).
39. Profos, P.: Stabilisation of flow distribution in forced-flow heating surfaces. Sulzer Tech. Rev. 4: 11–18 (1959).
40. Quandt, E.R.: Analysis and measurement of flow oscillations. Chem. Eng. Prog. Symp. Ser. 32, 57: 111–126 (1971).
41. Rizwan-uddin, Dorning, J.J.: Some nonlinear dynamics of a heated channel. Nucl. Eng. Des. 93: 1–14 (1986).
42. Rizwan-uddin, Dorning, J.J.: A chaotic attractor in a periodically forced two-phase system. Nucl. Sci. Eng. 100: 393–404 (1988).
43. Roy, R.P., Su, M.-G., Dykhuizen, R.C., Kalra, S.P.: Frequency response of boiling flow systems based on a two-fluid model. Int. J. Heat Mass Transfer 29: 1349–1357 (1986).
44. Saha, P., Ishii, M., Zuber, N.: An experimental investigation of the thermally induced flow oscillations in two-phase systems. J. Heat Transfer 98: 616–622 (1976).
45. Saha, P. Zuber, N.: An analytical study of the thermally induced two-phase flow instabilities including the effect of thermal non-equilibrium. Int. J. Heat Mass Transfer 21: 415–426 (1978).
46. Seward, P.E.: A two-fluid model for the analysis of gross flow instabilities in boiling systems. D.Ph. thesis, University of Oxford, Oxford, U.K. (1995).
47. Wallis, G.B., Heasley, J.H.: Oscillations in two-phase flow systems. J. Heat Transfer 83: 363–369 (1961).
48. Whalley, P.B.: Boiling, condensation and gas-liquid flow. Oxford University Press, Oxford (1987).
49. Whitaker, S.: The transport equations for multi-phase systems. Chem. Eng. Sci. 28: 139–147 (1973).
50. Yadigaroglu, G., Bergles, A.E.: Fundamental and higher-mode density-wave oscillations in two-phase flow. J. Heat Transfer 94: 189–195 (1972).
51. Zuber, N.: Flow excursions and oscillations in boiling, two-phase flow systems with heat addition. In: Proceeding of the symposium on two-phase flow dynamics, Eindhoven, EUR 4288e, pp. 1071–1089 (1967).
52. Zuber, N., Finlay, J.A.: Average volumetric concentration in two-phase flow systems. J. Heat Transfer 87: 453–468 (1965).
53. Zuber, N., Staub, F. W.: The propagation and the wave form of the vapor volumetric concentration in boiling, forced convection system under oscillatory conditions. Int. J. Heat Mass Transfer 9: 871–895 (1966).
54. Zuber, N., Staub, F. W.: An analytical investigation of the transient response of the volumetric concentration in a boiling forced-flow system. Nucl. Sci. Eng. 30: 268–278 (1967).

Authors' addresses: C.J. Aldridge, Department of Mathematics, University of Strathclyde, Livingstone Tower, 26 Richmond Street, Glasgow G1 1XH, United Kingdom.—A.C. Fowler, OCIAM, Mathematical Institute, University of Oxford, Oxford, United Kingdom.